

Accepted manuscript doi: 10.1680/jgele.21.00053

Accepted manuscript

As a service to our authors and readers, we are putting peer-reviewed accepted manuscripts (AM) online, in the Ahead of Print section of each journal web page, shortly after acceptance.

Disclaimer

The AM is yet to be copyedited and formatted in journal house style but can still be read and referenced by quoting its unique reference number, the digital object identifier (DOI). Once the AM has been typeset, an 'uncorrected proof' PDF will replace the 'accepted manuscript' PDF. These formatted articles may still be corrected by the authors. During the Production process, errors may be discovered which could affect the content, and all legal disclaimers that apply to the journal relate to these versions also.

Version of record

The final edited article will be published in PDF and HTML and will contain all author corrections and is considered the version of record. Authors wishing to reference an article published Ahead of Print should quote its DOI. When an issue becomes available, queuing Ahead of Print articles will move to that issue's Table of Contents. When the article is published in a journal issue, the full reference should be cited in addition to the DOI.

Accepted manuscript doi: 10.1680/jgele.21.00053

Submitted: 18 May 2021

Published online in ‘accepted manuscript’ format: 13 September 2021

Manuscript title: An experimental investigation into the attractive forces controlling clay particles’ micromechanical interactions

Authors: L. P. de Morais*, A. Tarantino[†] and M. P. Cordão Neto*

Affiliations: *Department of Civil and Environmental Engineering, University of Brasília-UnB, Brasília, Brazil and [†]Department of Civil and Environmental Engineering, University of Strathclyde, Glasgow, UK

Corresponding author: Letícia Pereira de Morais, Campus Darcy Ribeiro, SG 12, Geotecnia, Brasília, Brazil.

E-mail: leticia.12.morais@gmail.com, 160105072@aluno.unb.br

Abstract

Modelling clay behaviour is a challenging task because many of microscopic features are still unknown including interparticle forces and particle association, which may explain the different behaviours of clay when subjected to hydro-mechanical loading. This paper presents an experimental study to investigate the micromechanical interactions of clay particles. Kaolinite samples were compacted to high vertical stresses and granulometry laser tests were carried out to investigate particle agglomeration. Samples were compacted in a dry state, with 10% water content and 10% dispersant solution content. The results show that loading generated agglomeration. Also, increasing vertical stress induced larger agglomeration. When comparing specimens compacted using different pore-fluids, the agglomeration process is more pronounced at high values of dielectric permittivity (water). We conclude that the association of particles forming agglomerates is due to van der Waals forces. This was mainly inferred from the observation that agglomeration occurred even when compacted samples were prepared with dispersant solution (which turns attractive coulombic forces into repulsive ones). This also indicates that association of particles occurs in face-to-face mode due to the high stress applied. The similar response of samples compacted with water and sodium hexametaphosphate solution and the ESEM images of compacted samples also show this type of arrangement. The comprehension of interparticle forces and particle associations can improve discrete modelling of fine-grained materials.

Keywords: Clays; Compaction; Particle-scale behaviour

Introduction

The mode of particle arrangement in clay geomaterials is important to understanding fundamental aspects of clay mechanical behaviour such as soil compressibility and shear strength. To study particle arrangement, it is important to understand interparticle forces, which may be used in the formulation of numerical discrete models where the nature of interparticle forces must be known. According to Santamarina (2001), particles in a granular medium are subjected to forces that can be classified as non-contact forces (distances exceeding $\sim 20 \text{ \AA}$) and contact forces at shorter distances (Born repulsion). In clay materials, non-contact electrical forces play a key role, and these include van der Waals and Coulombic forces. van der Waals forces are long distance forces that are associated with molecule polarization. The dipole moment is generated by asymmetric electron distribution within the molecule and can polarize another molecule to form attractive van der Waals forces. Coulombic forces are related to the presence of charges on clay particles. The presence of charges (positive or negative) mainly results from permanent changes in the structure of the particle lattice, such as isomorphous substitution and broken edges, and protonation and deprotonation reactions. The magnitude of van der Waals and Coulombic forces varies with the distance from the particle. At small distances, attractive van der Waals forces tend to overcome Coulombic forces. Coulombic forces dominate as distance increases.

van der Waals and Coulombic forces control particle association in clay soil. According to van Olphen (1977), particle association in suspension may be dispersed (no face-to-face particle association), aggregated (face-to-face particle association), flocculated (edge-to-face or edge-to-edge aggregate association), and deflocculated (no association between aggregates). Aggregates and agglomerates are commonly used as synonyms. Here, the terminology adopted by Taurozzi et al. (2011) will be used to distinguish agglomerates from aggregates. According to Taurozzi et al. (2011) agglomerates are assemblage of particles held together by weak forces (van der Waals, capillary, or electrostatic forces) in which particles may be separated by techniques such as sonication or high intensity mixing. Aggregates are particles strongly bonded together by interactions such as fusion, metallic bonds, etc.

Particle-scale behaviour is directly related to the distribution of charges around clay particles. Kaolinite particles may exhibit positive charges or negative charges on the surface depending on the pH of medium that is being studied. There is no consensus on the distribution of charges on kaolinite particles and the intensity of the surface charge. The traditional model assumes that particle faces are charged negatively whereas the particle edge is charged either positively or negatively depending on pH (Wang and Siu 2006; Pedrotti and Tarantino,

2018). Although the charge of the faces is generally associated with permanent charge due to isomorphous substitutions, Zhou & Gunter (1992) have suggested that the charge of the faces is also pH dependent. Traditional measurements of surface charge based on acid-base titration and cesium cation exchange capacity suggests that surface charge is of the order of a few hundredths of mC/m² (Schroth & Sposito 1997). This representation has been entirely overturned by recent measurements based on Atomic Force Microscope (AFM). Gupta & Miller (2010) and Liu et al. (2014) have measured always negative charge of the edge regardless of pH, negative charge of the silica face, and charge of the alumina face that goes for positive to negative values as pH increases. In addition, the measured surface charge of the order of only a few mC/m². In this paper, we followed the Utah model (Gupta & Miller, 2010; Liu et al. 2014). It should be noted, however, that despite the significant discrepancies between the two models, they both lead to the conclusion that particle charge is negative all around the particle at high pH whereas edge-to-face contacts can be activated at low pH due to face and edge oppositely charged.

Edge-to-face contacts occurring in acidic media will present a more open structure. In alkaline media, kaolinite particles are negatively charged on all surfaces, and no attractive coulombic forces are present. The competition between attractive and repulsive forces controls particle association and clay behaviour.

This paper aims to investigate attractive interactions between particles of compacted samples. Different conditions (stress, pore-fluid) were studied to understand interparticle forces and particle association. Morais et al. (2019) showed that agglomerations are mostly formed by face-to-face interactions (stacks) when high loads were applied. These interactions occur due to van der Waals or Coulombic forces. This paper also discusses the distribution of charges around kaolinite particles using different media in the tests.

2. Experimental Programme

Materials used

The material used in this study is a Kaolinite composed of 43.3% SiO₂ and 39.9% Al₂O₃. Liquid and plastic limits of samples prepared with distilled water as well as granulometry tests were performed to characterize the material. **Table 1** shows that the kaolinite used in this research compares favourably with other materials tested in the literature. The material's grain size distribution was obtained by laser granulometry tests (CILAS, model Microcurve). **Figure 1** presents the kaolinite grain size distribution.

Specimen preparation

Kaolinite samples were compacted at high stresses via static compaction. Compaction is expected to reduce particle distance and trigger attractive interactions. This generates agglomerates of particles either by van der Waals and/or Coulombic interactions. High stress compaction was achieved by applying vertical stresses of 2 MPa (dry powder) and 100 MPa (dry powder, 10% water content and 10% dispersant solution content). The vertical stress was maintained for 15 minutes, and a minimum porosity of 27% was achieved at 100 MPa). Samples with 10% water content were prepared the day before the test for moisture homogenization. The water content was very low, and we assumed that there was no consolidation process ($S_r < 71\%$). The dispersant solution consisted of sodium hexametaphosphate solution (45.7 g of sodium hexametaphosphate to 1000 L of distilled water).

Laser Granulometry tests

Grain size distribution was measured via laser granulometry tests and aimed to investigate the agglomeration process and particle interactions. Laser granulometry tests of compacted samples were performed with and without the use of ultrasound (mechanical stirring) during the test (Chappell, 1998). Two techniques were used to prepare the sample for laser granulometry test: compacted kaolinite was left immersed in either distilled water or in an experimental dispersant solution for 24 hours before the test. **Table 2** presents all combinations of tests performed. Sonication is highly effective in destroying agglomerations caused by van der Waals interactions (Taurozzi et al., 2011). The dispersant solution (sodium hexametaphosphate solution) was used to investigate the role of coulombic attractive interactions because it turns attractive interactions into repulsive ones and hence disassociates particles. ESEM imaging was performed on compacted samples for direct observation of microscopic fabric.

3. Results and Discussion

To better visualize and understand the results, a symbology was used to illustrate the procedure adopted in the laser granulometry test (**Table 2**). In the name of the samples, the letters W and N, standing for With and No/without respectively, correspond to the use and no use of a technique, respectively. The first letter corresponds to dispersant solution immersion before laser granulometry and the second letter to ultrasound during laser granulometry. For example, sample Powder-N-W is a kaolinite powder without the immersion in dispersant solution and with the use of ultrasound.

Figure 1 presents the grain size distribution of kaolinite powder. In this study, the true size distribution is attributed to the curve of the powder where ultrasound and immersion in dispersant solution are presented (Powder-W-W). The true size distribution curve overlaps with the curve obtained when only the dispersant solution was used (Powder-W-N). The powder shows some agglomerates when no dispersant solution is used, regardless of whether ultrasound is used (Powder-N-W) or ultrasound is not used (Powder-N-N). The effect of the dispersant solution suggests that Coulomb attractive interactions are present in the powder. On the other hand, the ultrasound having no effect on the distribution of the powder suggests that van der Waals forces do not play any significant role in the powder (at zero stress).

Figures 2, 3, 4 and 5 show the grain size distribution of samples statically compacted to 2 MPa (dry powder, 2D), 100 MPa (dry powder, 100D), 100 MPa (10% water content, 100W), and 100 MPa (10% dispersant solution content, 100H) respectively. Curves of these samples present the same behaviour: Ultrasound is more effective in dissociation of particles as observed in the curves i) without immersion in dispersant solution and with ultrasound (N-W) and ii) with immersion in dispersant solution and with ultrasound (W-W). This is demonstrated by the curves associated with ultrasound treatment shifting to the left. The use of immersion in dispersant solution before laser granulometry tests was studied in the curves with dispersant solution and without ultrasound (W-N); there was no effect on the agglomeration as these curves match the no-treatment curve. This suggests that columbic attractive forces do not play any significant role in agglomeration and hence particle interactions as the stress is progressively increased.

Figure 6 presents all curves W-N for 2 MPa, 100 MPa with 10% of dispersant solution content, and 100 MPa with 10% of water content. Increasing loading shifts the curves to the right meaning that more attractive interactions are activated. Although attractive forces are activated in all compacted samples, their response to ultrasound and immersion in dispersant solution is different. Ultrasound treatment affected the agglomerations formed by all samples (W-W and N-W curves) as observed in **Figure 3, 4 and 5**, but the immersion in dispersant solution during preparation had no effect on the agglomerations. According to Lagaly (1989), the dispersant solution provides anions that are adsorbed by the surface and increase the negative surface charge thus dispersing the particles. It also increases the pH of the dispersion, which produces alkaline medium that changes the particle surface charges from positive to negative. The ultrasound will mechanically disaggregate particles as it causes the rapid movement of the liquid due to transmission of sound waves (Taurozzi et al., 2011). Both methods may be used to disaggregate particles, but one approach might be more effective than the

other depending on the attractive forces mainly responsible for particle agglomeration, i.e., either van der Waals or columbic forces.

Figure 7 compares samples without any treatment. Samples 100D-N-N and 100W-N-N show that water produces larger particle agglomerates. Water has a dielectric permittivity higher than air thus reducing repulsive coulombic forces between particles and increasing the net attractive forces. Although more agglomerations are formed, they have the same nature as observed in the response to immersion in dispersant solution and ultrasound. **Figure 7** also shows that sample 100H-N-N has agglomerations. The use of dispersant solution during compaction will change particle surface charge from positive to negative, and Coulombic interactions go from attractive to repulsive. If the agglomerations were due to Coulombic forces, then this compaction would not generate agglomerations. As agglomerates are observed, the main interaction between particles is due to van der Waals forces (face-to-face). Moreover, it can be observed that the curves associated with dry compaction (100D-N-N) and 10 % dispersant solution content (100H-N-N) respectively, although close, show some differences suggesting that forces controlling agglomeration are different. In air, particle interactions are controlled by van der Waals forces and both attractive and repulsive coulombic forces. In dispersant solution, particle interactions are controlled by van der Waals forces and just repulsive coulombic forces. In addition, the permittivity of dispersant solution is closer to the permittivity of water and repulsive interactions are reduced in dispersant solution when compared to the case where the pore-fluid is air.

Table 3 presents schematically the interaction between kaolinite particles depending on the pore-fluid at compaction (water or dispersant solution). According to the distribution of charges around clay particles presented by Gupta & Miller (2010) and Liu et al. (2014), it is possible to explain why the curves of samples compacted with water and dispersant solution do not overlap despite their dielectric permittivity values being very close. In water, the kaolinite alumina (octahedral) face is positive, and the silica (tetrahedral) face is negative. Coulombic face-to-face interactions can therefore be either attractive or repulsive depending on whether faces of the same or opposite charge face each other. In the dispersant solution, the surface charge is negative on both faces, and coulombic face-to-face interactions are always repulsive. When a high stress is applied, more energy needs to be spent to overcome repulsive interactions in dispersant solution, and smaller agglomerations are observed in contrast with samples compacted with water.

The mode of particle associations can also be discussed. First, the level of stress applied (MPa) is so high that sliding is very likely to occur at most edge-to-face contacts, which would therefore be 'broken' mechanically as observed by Pedrotti (2016). Several works about particles orientation (Dejran-Maigre et al., 1998; Hattab and Fleureau, 2010; Chow et al., 2019) show that particles tend to orient with increasing loading, and edge-to-face contacts tend to disappear. In addition, the assumption that particles are arranged in face-to-face configuration explains the different behaviour observed for 100W-N-N and 100H-N-N as explained above (**Table 3**).

Figure 8 presents the ESEM images of samples compacted dry (100D), with water (100W), and dispersant solution (100H) respectively up to 100MPa. Agglomerations are formed by face-to-face associations (no edge-to-face associations are observed) and there seems to be little or no differences between the three samples. This confirms the above assumption that very high stresses break edge-to-face contacts and force the particles to align orthogonal to the direction of loading in face-to-face association. The only difference that would be expected is the one discussed in Table 3 but this is difficult to observe from these images.

4. Conclusions

This paper has explored the role of van der Waals and columbic attractive forces in controlling particle interaction. van der Waals are always present and generate attraction provided mechanical energy brings them at very close distance (in the range of tenths of nanometers). Attractive columbic forces are active only in acidic pore-water where edge and faces are oppositely charged. Acidic conditions are generally achieved with standard tap or demineralised water and are therefore relevant in soil mechanics. While the role of van der Waals and columbic attractive forces have been widely recognised and discussed in colloidal science, there has been little or no investigation on their role in consolidated clays, which are the focus of soil mechanics. This question is relevant for discrete numerical modelling because it allows for convenient design of interparticle interaction forces or potential energy.

The first research questions addressed in this work is how to discriminate agglomeration due to van der Waals or columbic attractive forces. It has been shown that the use of ultrasound and sodium hexametaphosphate in laser granulometry allows for discriminating these two attractive forces.

The second research question concerned the role of van der Waals and columbic attractive forces. In a nutshell, van der Waals forces do not appear to have any role in particle agglomeration at zero stress (powder in suspension) whereas van der Walls forces are the only forces responsible for agglomeration at stresses $\geq 2\text{MPa}$. It can be speculated that in the stress range 0-2MPa the attractive columbic forces are progressively becoming less important as the stress increases until not playing any role at all.

More in detail, the main conclusions can be summarised as follows:

- Two mechanisms of attractive interactions are observed: Coulombic interactions are observed in powder at zero stress (Powder-N-N curve) whereas van der Waals interactions are observed when particles are brought together by loading.
- van der Waals interactions are activated more and more with increasing stress as observed when the laser granulometry curve 2D-W-N is compared with 100H-W-N and 100W-W-N. The van der Waals interactions are likely to be more active when the permittivity of the pore-fluid is higher and, hence, repulsive Coulombic forces are smaller as observed from the comparison of laser granulometry curves of samples compacted dry (100D-N-N) and at 10% water content (100W-N-N) to 100 MPa
- The distribution of charges around the clay surface reflects on the agglomeration process as observed from the difference between laser granulometry curves of dispersant solution compaction (100H-N-N) and water compaction (100W-N-N). Considering that the permittivity values of dispersant solution and water are similar, the main difference between the two samples are the charges around clay particle, which are negative on all faces and edge when clay is compacted with the dispersant solution.
- Finally, the surface charge model presented by Gupta & Miller (2010) and Liu et al. (2014) appears to be consistent with the different response observed when using either water or dispersant solution as fluid at compaction.

Acknowledgements

The authors acknowledge the financial and technical support provided by the European Commission by Marie Curie IRSES project GREAT (FP7-PEOPLE-2013-IRSES-612665), by the “Conselho Nacional de Desenvolvimento Científico e Tecnológico” CNPq of Brazil, “Fundação de Apoio à pesquisa” FAP-DF of Brazil, University of Brasília, University of Los Andes, the FURNAS laboratory, and LMM-UnB Laboratory.

List of notations

Sr is the saturation

References



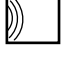


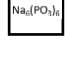
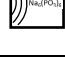
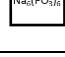
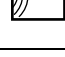

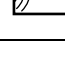
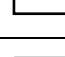
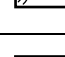
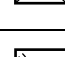
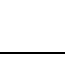

- Chappell A (1998) Dispersing sandy soil for measurement of particle size distributions using optical laser diffraction. *Catena* 31: 271-281.
- Chow JK, Li Z, Wang Y-H (2019) Comprehensive microstructural characterizations of 1-D consolidated kaolinite samples with fabric tensors and pore elongation factors. *Engineering Geology* 248: 22-33.
- Dejran-Maigre I, Tessier D, Grunberger D, Velde B, Vasseur G (1998) Evolution of microstructures and of macroscopic properties of some clays during experimental compaction. *Marine and Petroleum Geology* 15: 109-128.
- Gupta V and Miller JD (2010) Surface force measurements at the basal planes of ordered kaolinite particles. *Journal of Colloid and Interface Science* 344: 362-371.
- Hattab M and Fleureau J-M (2010) Experimental study of kaolin particle orientation mechanism. *Geotechnique* 60, No. 5 : 323-331.
- Lagaly G (1989) Principles of Flow of Kaolin and Bentonite Dispersions. *Applied Clay Science* 4: 105-123.
- Liu J, Sandaklie-Nikolova L, Wang X, Miller JD (2014) Surface Force Measurements at Kaolinite Edge Surfaces Using Atomic Force Microscopy. *Journal of Colloid and Interface Science* 420: 35-40.
- Mesri G, Olson R E (1971) Mechanism Controlling the permeability of clay. *Clays and Clay Minerals* 19 :151-158
- Morais LM, Cordão-Neto M, Tarantino A (2019) Aggregation process of kaolinite clay. In Proceedings of 7th International Symposium on Deformation Characteristics of Geomaterials, Glasgow, UK.
- Pedrotti M (2016) An experimental investigation on the micromechanisms of non-active clays in saturated and partially saturated states. PhD Thesis, University of Strathclyde, Glasgow, UK.

- Pedrotti M, Tarantino A (2018) An experimental investigation into the micromechanics of non-active clays. *Geotechnique* 68, No 8: 666-683
- Santamarina JC (2001) Soil Behavior at the Microscale: Particle Force. Symposium on Soil Behavior and Soft Ground Construction Honoring Charles C. "Chuck" Ladd. Cambridge, Massachusetts, USA.
- Sasanian S, Newson T A (2013) Use of mercury intrusion porosimetry for microstructural investigation of reconstituted clays at high water contents. *Engineering Geology* 158: 15-22
- Sridharan A, Venkatappa Rao G (1973) Mechanisms controlling volume change of saturated clays and the role of the effective stress concept. *Geotechnique* 23, No 3: 359-382
- Schroth, B & Sposito, G. 1997. Surface Charge Properties of Kaolinite. *Clays and Clay Minerals*, 45(1): 85-91.
- Taurozzi JS, Hackley VA and Wiesner MR (2011) Ultrasonic dispersion of nanoparticles for environmental, health and safety assessment- issues and recommendations. *Nanotoxicology* 5(4): 711-729.
- van Olphen (1977) *An Introduction to Clay Colloid Chemistry*. Wiley-Interscience, New York, USA.
- Wang, Y-H & Siu, W. (2006). Structure characteristics and mechanical properties of kaolinite soils. I. Surface charges and structural characterizations. *Canadian Geotechnical Journal*. 43. 587-600. 10.1139/t06-026.
- Zhou Z, Gunter WD. 1992. The nature of the surface charge of kaolinite. *Clays Clay Miner* 40:365-368

Table 1. Atterberg limits for kaolinite clay.

	Liquid limit (%)	Plastic limit (%)
This work	49-51	35-41
Mesri and Olson (1971)	40-50	27-31
Sridharan and Rao (1973)	49	29
Sasanian and Newson (2013)	61	36
Pedrotti and Tarantino (2018)	64	32

Table 2. Tests performed.

Sample Name	Preparation method	Vertical stress (MPa)	Dry density (g/cm^3)	Investigation method	Symbol
Powder-W-W	Dry Powder-no preparation	-	-	Laser granulometry- with dispersant and with ultrasound	
Powder-W-N	Dry Powder-no preparation	-	-	Laser granulometry- with dispersant and without ultrasound	
Powder-N-W	Dry Powder-no preparation	-	-	Laser granulometry- without dispersant and with ultrasound	
Powder-N-N	Dry Powder-no preparation	-	-	Laser granulometry- without dispersant and without ultrasound	
2D-W-W	Static Compaction-dry	2	1,040	Laser granulometry- with dispersant and with ultrasound	
2D-W-N	Static Compaction-dry	2	1,040	Laser granulometry- with dispersant and without ultrasound	
100H-W-W	Static Compaction-10% dispersant	100	1,863	Laser granulometry- with dispersant and with ultrasound	
100H-W-N	Static Compaction-10% dispersant	100	1,863	Laser granulometry- with dispersant and without ultrasound	
100H-N-W	Static Compaction-10% dispersant	100	1,863	Laser granulometry- without dispersant and with ultrasound	
100H-N-N	Static Compaction-10% dispersant	100	1,863	Laser granulometry- without dispersant and without ultrasound	
100D-W-W	Static Compaction-dry	100	1,877	Laser granulometry- with dispersant and with ultrasound	
100D-W-N	Static Compaction-dry	100	1,877	Laser granulometry- with dispersant and without ultrasound	
100D-N-W	Static Compaction-dry	100	1,877	Laser granulometry- without dispersant and with ultrasound	
100D-N-N	Static Compaction-dry	100	1,877	Laser granulometry- without dispersant and without ultrasound	
100W-W-W	Static Compaction-10% water content	100	1,847	Laser granulometry- with dispersant and with ultrasound	
100W-W-N	Static Compaction-10% water content	100	1,847	Laser granulometry- with dispersant and without ultrasound	



100W-N-W	Static Compaction- 10% water content	100	1,847	Laser granulometry- without dispersant and with ultrasound	
100W-N-N	Static Compaction- 10% water content	100	1,847	Laser granulometry- without dispersant and without ultrasound	

Table 3. Kaolinite Interactions in different media.

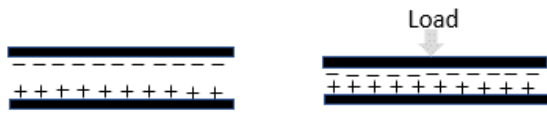
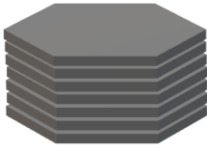


Fluid of compaction	Charges distribution around particles	Stacks
Water		
HMP solution		

Figure caption list

Figure 1. Grain size distribution of Kaolinite powder with different treatments.

Figure 2. Grain size distribution of samples compacted dry to 2 MPa with different treatments.

Figure 3. Grain size distribution of samples compacted dry to 100 MPa with different treatments.

Figure 4. Grain size distribution of samples compacted at 10% water content to 100 MPa with different treatments.

Figure 5. Grain size distribution of samples compacted at 10% dispersant solution content to 100 MPa with different treatments.

Figure 6. Comparison of grain size distribution of samples loaded to 2 MPa dry, 100 MPa with 10% water content, and 10% dispersant solution content.

Figure 7. Comparison of samples loaded to 100 MPa dry, with 10% water content, and with 10% dispersant solution content (N-N).

Figure 8. Electronic microscopic images compacted sample (a) 100D, (b)100W, and (c) 100H. Images are taken on a plane orthogonal to the direction of loading.

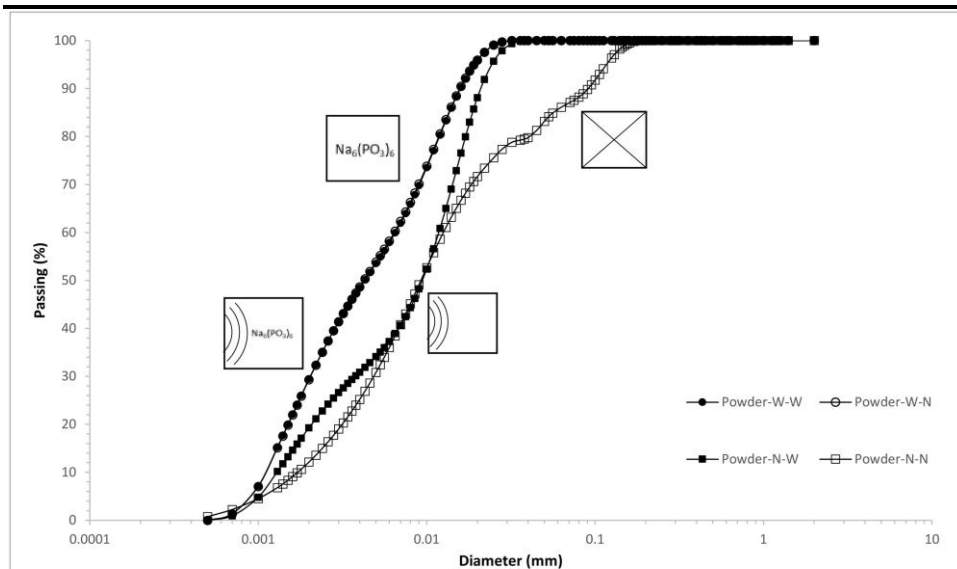


Figure 1.

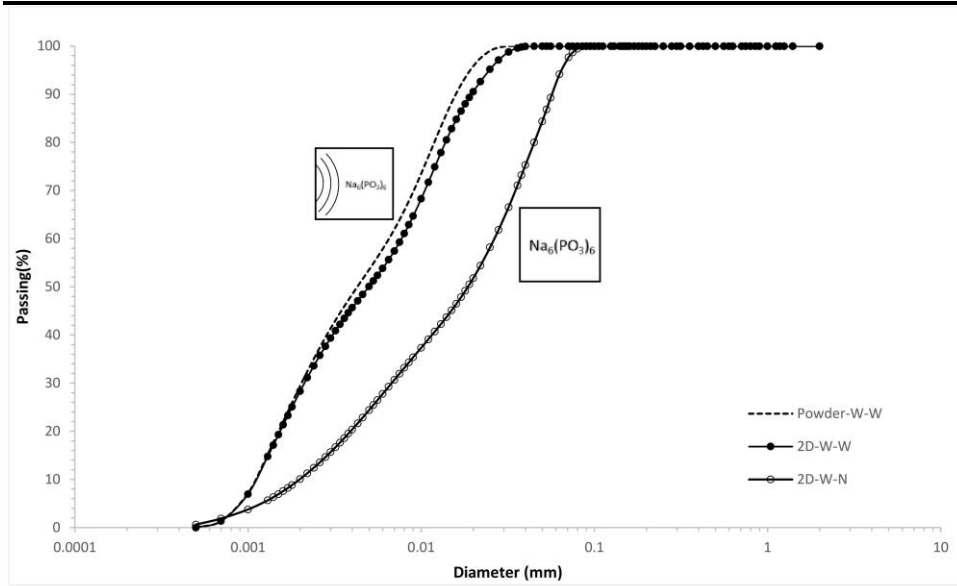


Figure 2.

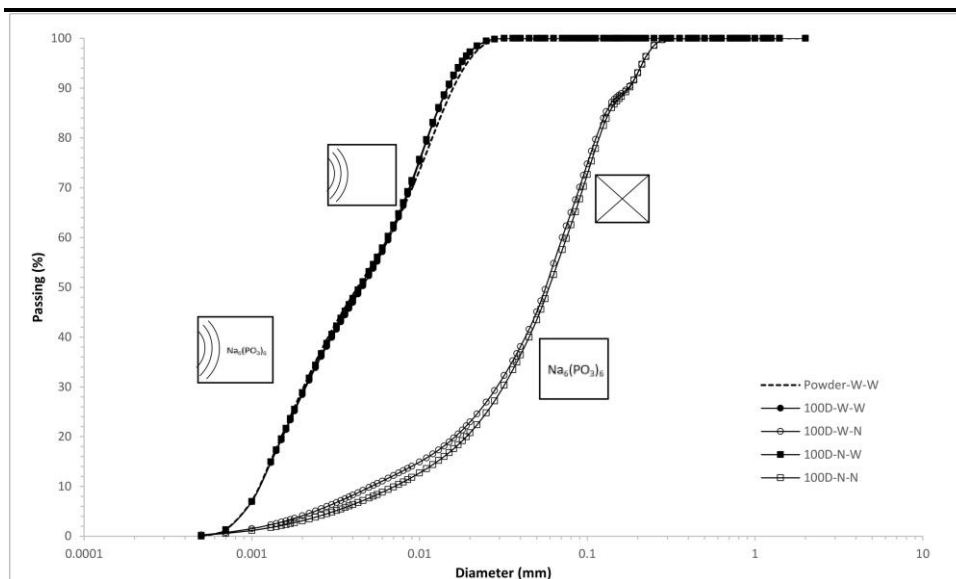


Figure 3.

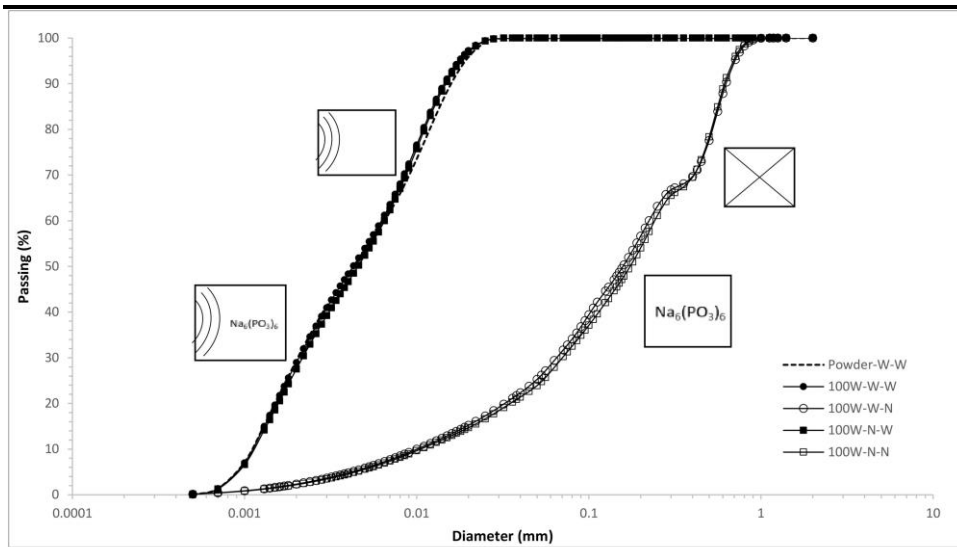


Figure 4.

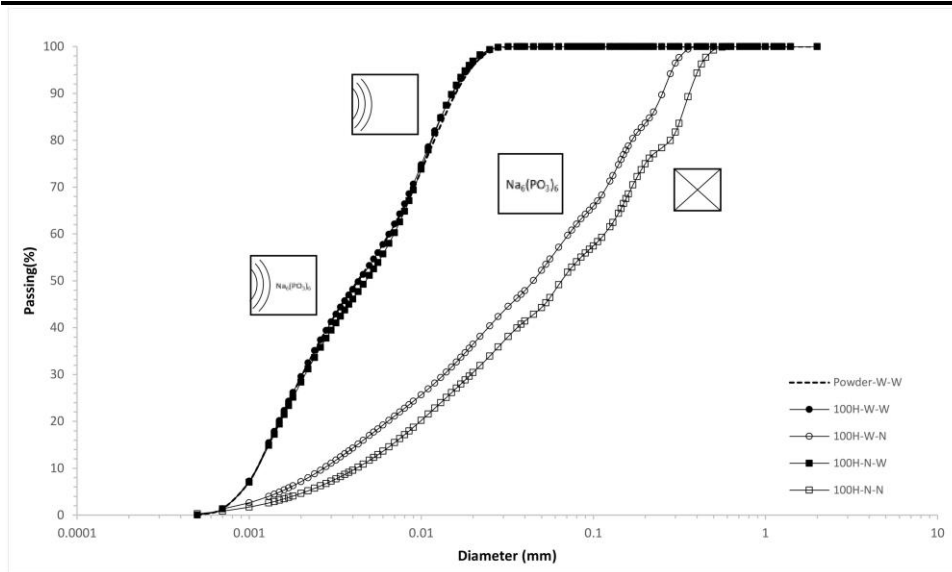


Figure 5.

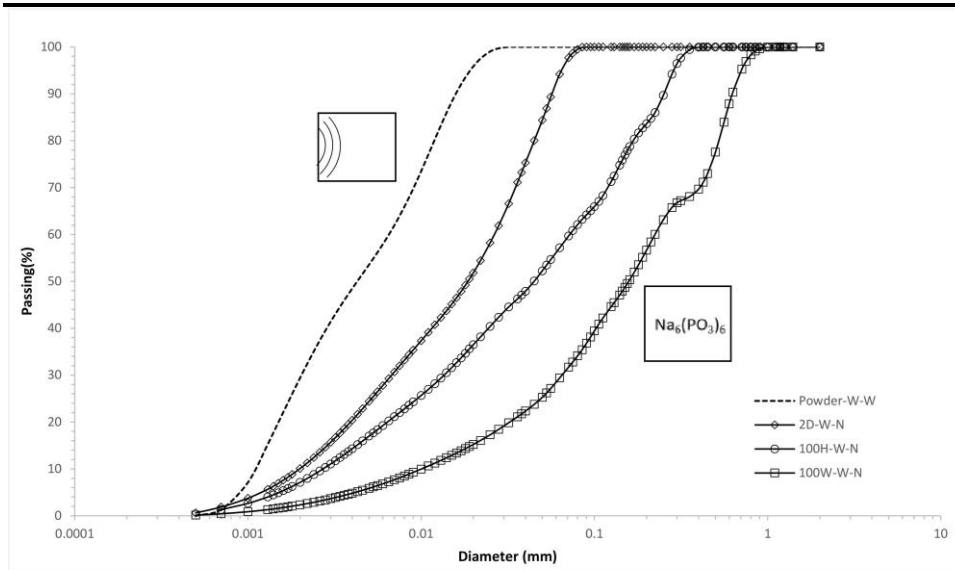


Figure 6.

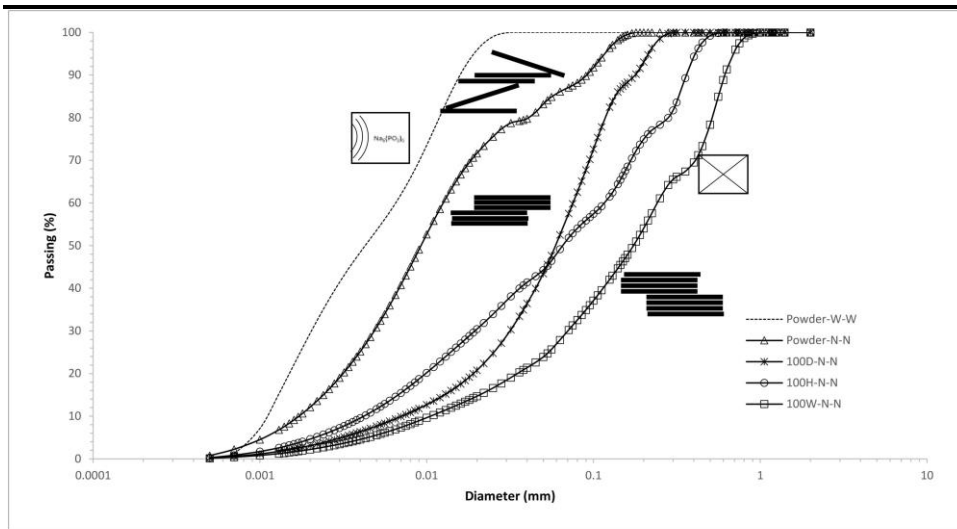


Figure 7.

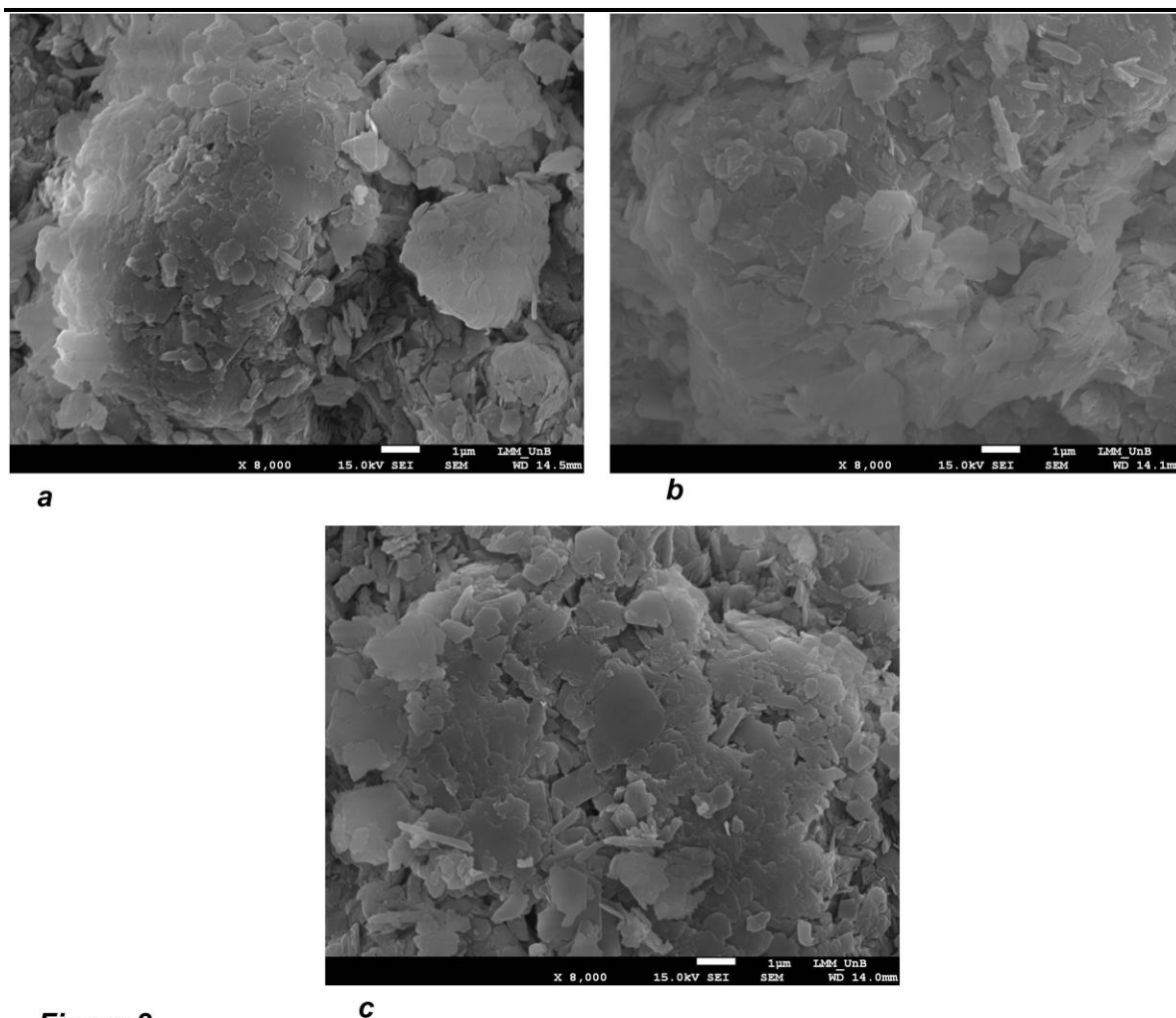


Figure 8

c